

Electronic Supplementary Information for

**All-visible-light triggered solid-state dual-color fluorescence
switching of phenanthroimidazole-based bisthiienylethene**

Qing Yan^a, Zhu Qiao^{a,b}, Weizhen Zhao^c, Jun Ren^{b*}, Yun Wang^a, Wanmei Yang^a,

Sheng Wang^{ab*}

^a School of Chemistry and Chemical Engineering, Key Laboratory of Clean Energy Materials Chemistry of Guangdong Higher Education Institutes, Lingnan Normal University, Zhanjiang, 524048, China. E-mail: dyesws@126.com.

^b Ministry of Education Key Laboratory for the Synthesis and Application of Organic Functional Molecules & Hubei Collaborative Innovation Center for Advanced Organic Chemical Materials, Hubei University, Wuhan, 430062, P.R. China. E-mail: renjun@hubu.edu.cn.

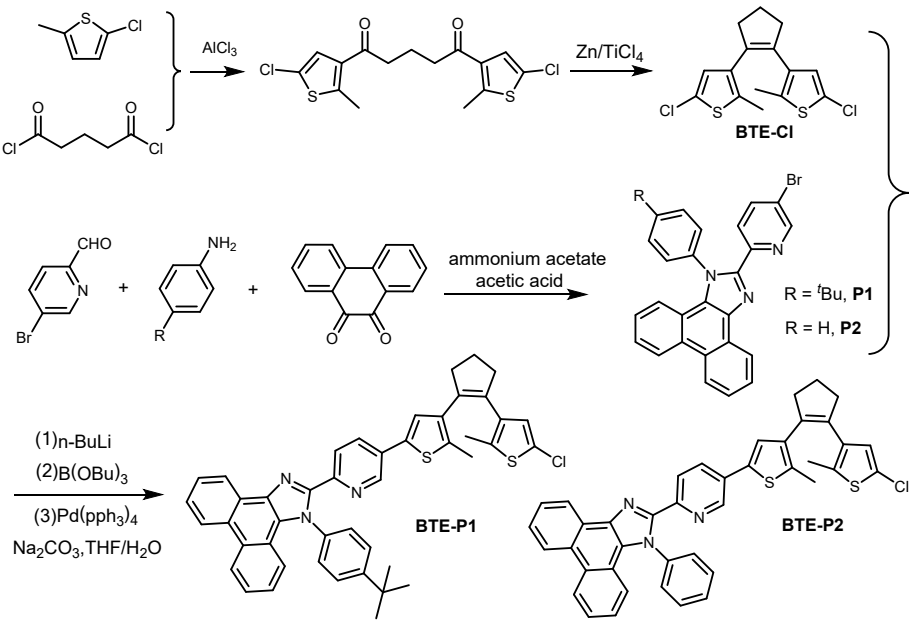
^c Beijing Key laboratory of Ionic Liquids Clean Process, Institute of Process Engineering, Chinese Academy of Sciences, Beijing 100190, P. R. China.

Table of content

1. Synthesis of products BTE-P1 and BTE-P2 -----	S1
2. Photochromism and fluorescence switching of BTE-P1 and BTE-P2 -----	S2
3. All-visible-light patterning application for information storage-----	S6
4. X-ray crystallographic analysis for BTE-P1 -----	S7
5. DFT theoretical calculations of BTE-P2 -----	S14
6. Size and Photophysical properties of BTE-P1@DSPE-PEG2000 -----	S15
7. Appendix: NMR spectra-----	S16
8. References-----	S19

1. Synthesis of product BTE-P1 and BTE-P2

The synthetic route for target products **BTE-P1** and **BTE-P2** are illustrated in Scheme S1. Compound **BTE-Cl** was prepared according to our previous literature.^[1] Compound **P1** and **P2** was prepared through Debus-Radziszewski imidazole synthesis.^[2]



Scheme S1 Synthetic routs of **BTE-P1** and **BTE-P2**.

2. Photochromism and fluorescence switching of BTE-P1 and BTE-P2.

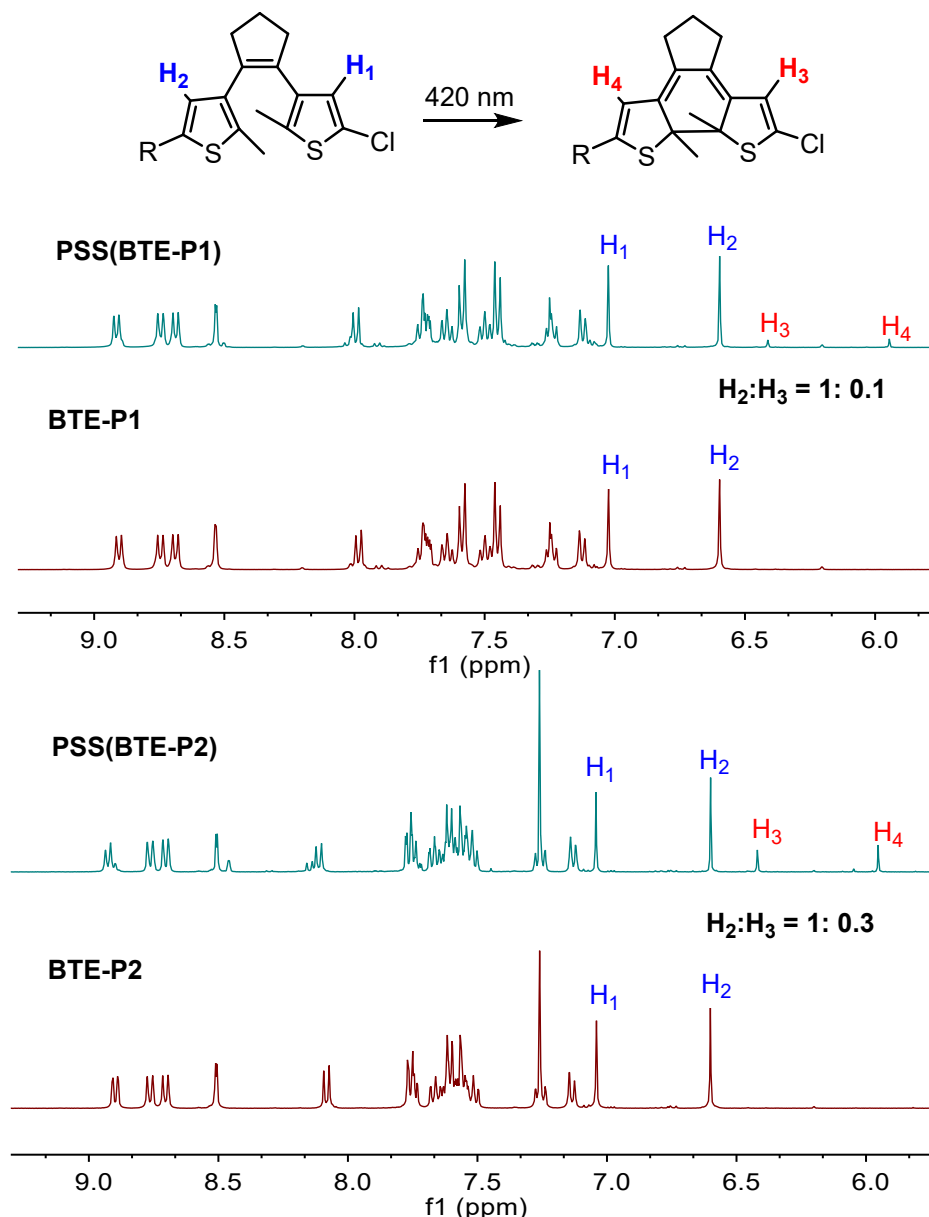


Fig. S1 Partial ¹H NMR spectra changes of **BTE-P1** and **BTE-P2** with 420 nm light irradiation in CDCl₃ at room temperature.

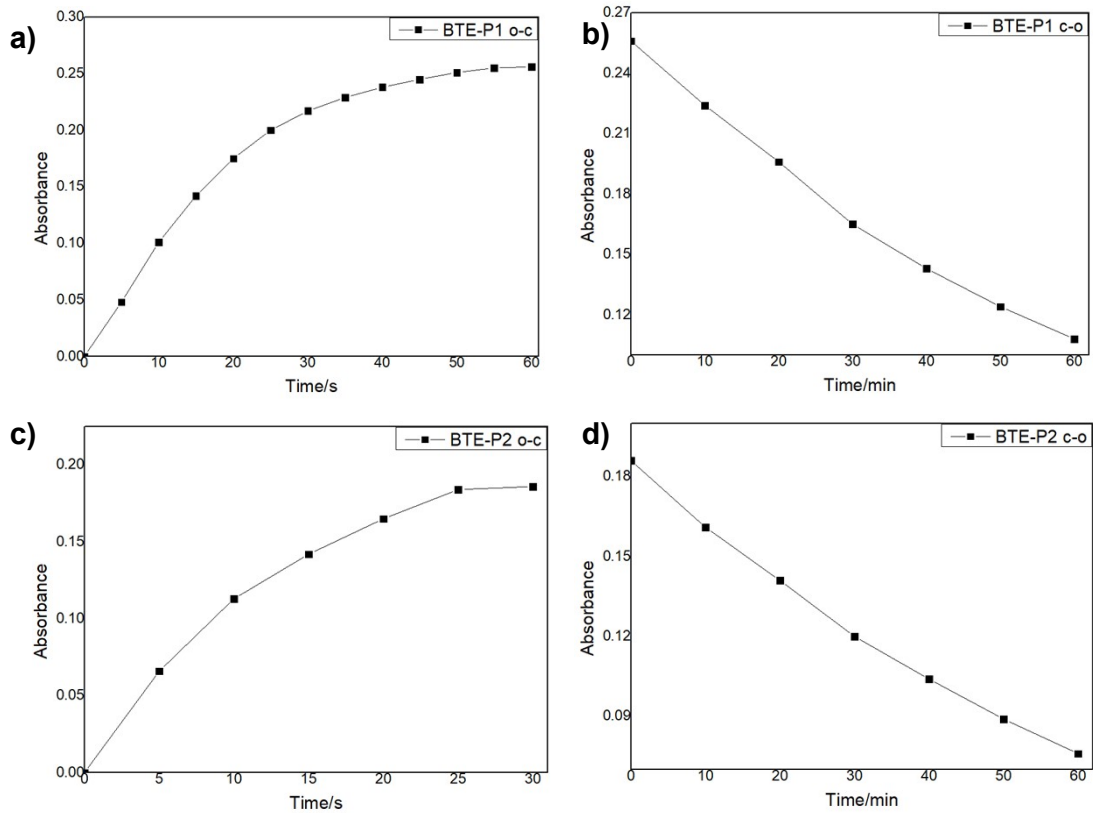


Fig. S2 Absorbance changes of **BTE-P1** upon irradiation with 310 nm (a) and 520 nm (b) in THF (1.0×10^{-5} M) monitored at 518 nm for ring-closed isomers. Absorbance changes of **BTE-P2** upon irradiation with 310 nm (c) and 520 nm (d) in THF (1.0×10^{-5} M) monitored at 517 nm for ring-closed isomers.

Table S1. Photochromic parameters of **BTE-P1** and **BTE-P2** in THF (1.0×10^{-5} M), respectively.

Name	Open		PSS		φ		Conversion ratio ^e (%)
	$\lambda_{\max}^{\text{a}}/\text{nm}$	$\varepsilon/(\text{M}^{-1}\text{cm}^{-1})$	$\lambda_{\max}^{\text{b}}/\text{nm}$	$\varepsilon/(\text{M}^{-1}\text{cm}^{-1})$	$\varphi_{\text{o-c}}^{\text{c}}$	$\varphi_{\text{c-o}}^{\text{d}}$	
BTE-P1	375	5.62×10^4	518	2.56×10^4	0.30	0.01	9
BTE-P2	374	4.68×10^4	517	1.86×10^4	0.40	0.02	23

^aAbsorption maxima of ring-open isomers. ^bAbsorption maxima of ring-closed isomers. ^cCyclization quantum yields($\varphi_{\text{o-c}}$). ^dCycloreversion quantum yields ($\varphi_{\text{c-o}}$).

^eConversion ratio was calculated through ^1H NMR of PSS.

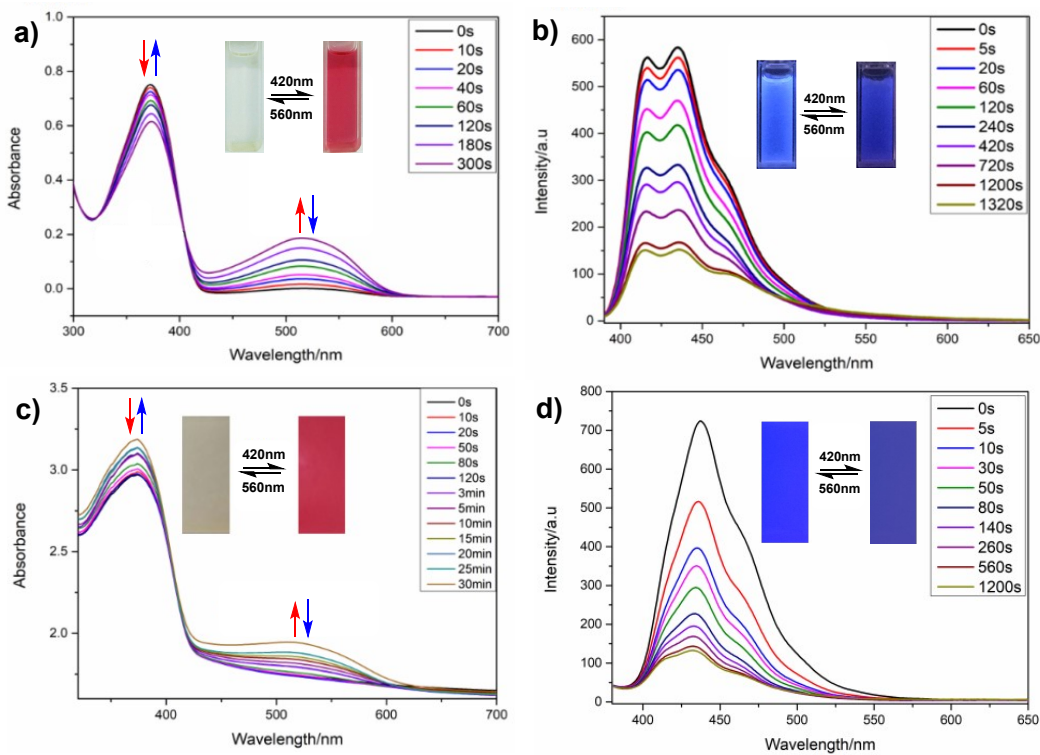


Fig. S3 The absorption and emission spectra changes of **BTE-P2** in THF solution or PMMA film under alternate 420 nm/550 nm irradiation. Inset: corresponding color and fluorescence changes of **BTE-P2** before and after irradiation. **a)** Absorption spectra changes in THF solution. **b)** Fluorescence spectra in THF solution. **c)** Absorption spectra changes in PMMA film. **d)** Fluorescence spectra in PMMA film.

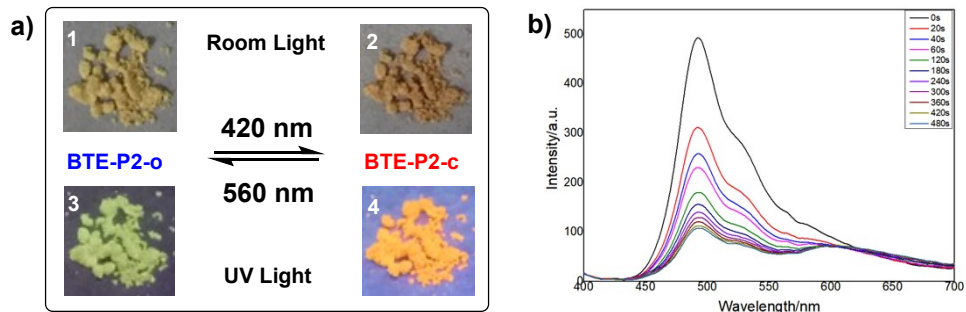


Fig. S4 The photochromism and fluorescence switching of **BTE-P2** in solid state under alternate 420 nm/560 nm irradiation. **a)** Corresponding color and fluorescence changes of **BTE-P2** (insets 1-4) before and after irradiation. **b)** Fluorescence spectra changes of **BTE-P2**.

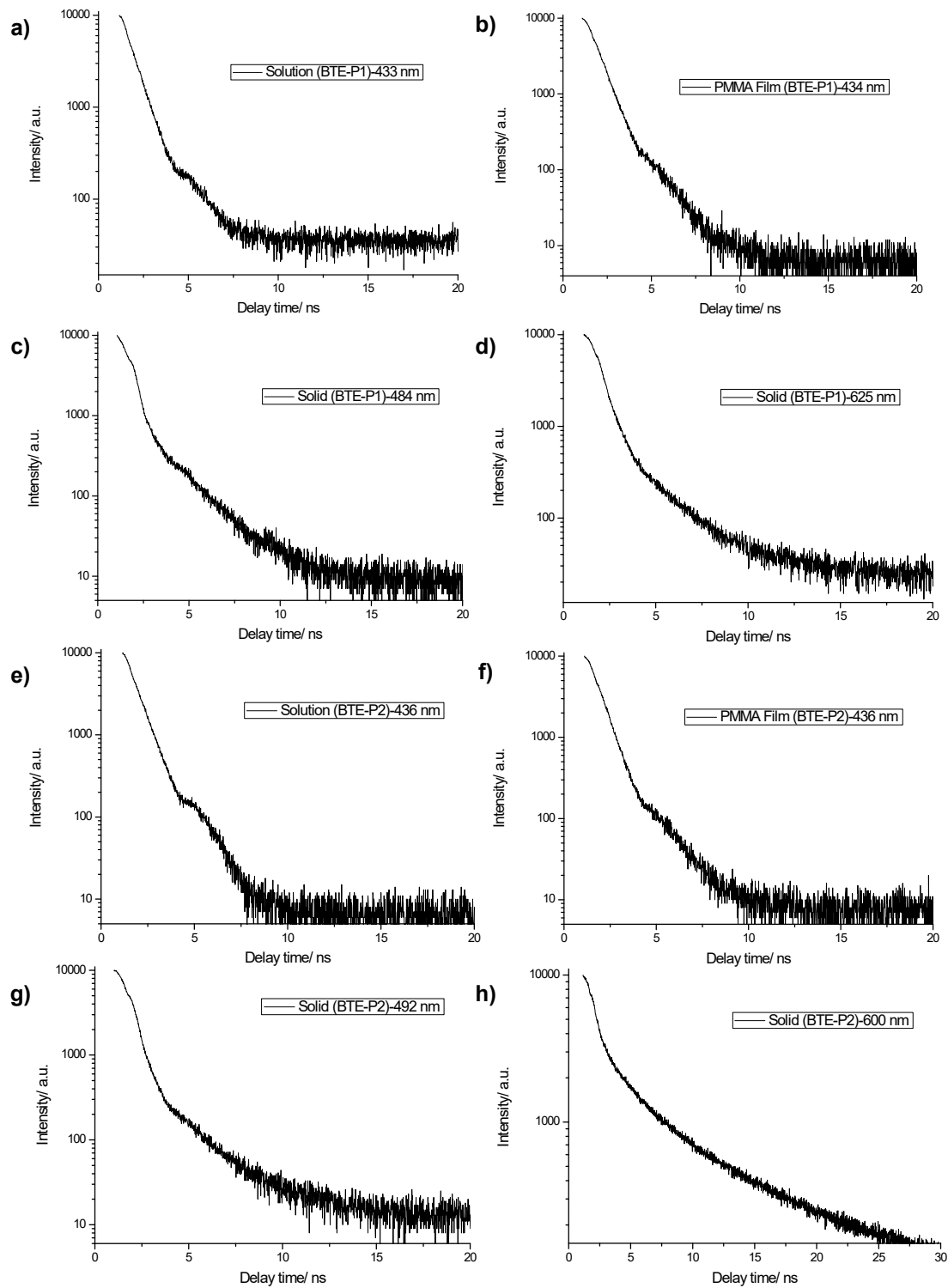


Fig. S5 Fluorescence decay curves of **BTE-P1** in THF solution (a), PMMA films (b), and solid state (c, d). Fluorescence decay curves of **BTE-P2** in THF solution (e), PMMA films (f), and solid state (g, h). The excitation wavelength was 405 nm.

Table S2. Fluorescence parameters of **BTE-P1** and **BTE-P2** in different state.

Name	State	λ_{em} (nm)	$\Phi_{F1}^{\text{a}} [\%]$ (open)	$\Phi_{F2}^{\text{a}} [\%]$ (PSS)	τ_1^{b} (nm)	τ_2^{b} (nm)
BTE-P1	Solution ^c	433	9.73	0.05	0.68	2.00
	PMMA film	434	8.25	0.12	0.73	2.26
	Solid	484			0.61	2.67
		625	16.30	7.18	0.75	3.53
BTE-P2	Solution ^c	436	7.67	0.03	0.64	1.60
	PMMA film	436	7.23	0.24	0.69	2.45
	Solid	492			0.69	3.79
		600	15.61	6.33	1.00	6.31

^aFluorescence quantum yield (excitation wavelength = 405 nm). ^bFluorescence Lifetime (excitation wavelength = 405 nm). ^cin THF solution (1.0×10^{-5} M).

3. All-visible-light patterning application for information storage.

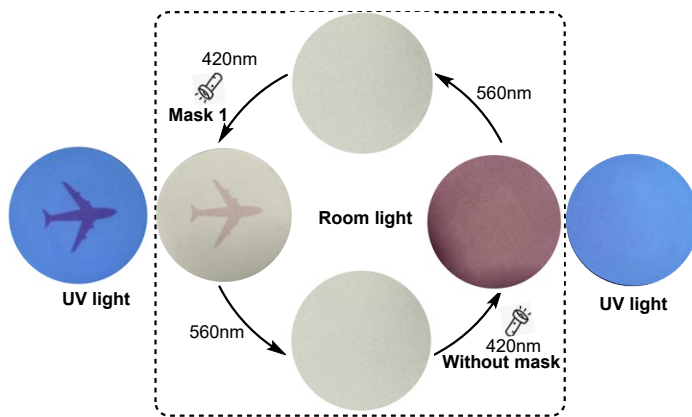


Fig. S6. All-visible-light patterning application of **BTE-P2** on a filter paper. A series of images were sequentially written onto and erased from the same filter paper with 420 nm/560 nm irradiation, respectively.

4. X-ray crystallographic analysis for BTE-P1.

single crystals of **BTE-P1** was prepared by slow evaporation of their dichloromethane/ethyl acetate/hexane mixed solutions. Single crystal X-ray crystallographic analysis was conducted on a Bruker APEX-II CCD diffractometer with graphite-monochromated MoK α radiation ($\lambda = 0.71073 \text{ \AA}$) at 273(2) K. The crystal structure was solved by a direct method and refined by the full-matrix least-squares on F^2 using SHELXL-2014 in Olex 2 software. Crystallographic data for the structure in this paper have been deposited with the Cambridge Crystallographic Data Centre as supplemental publication CCDC 2021742.

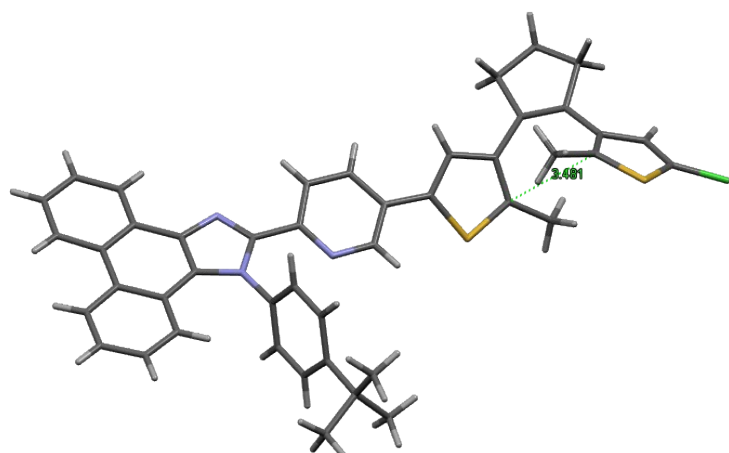


Fig. S7. The intramolecular distance between two reactive carbons in **BTE-P1**.

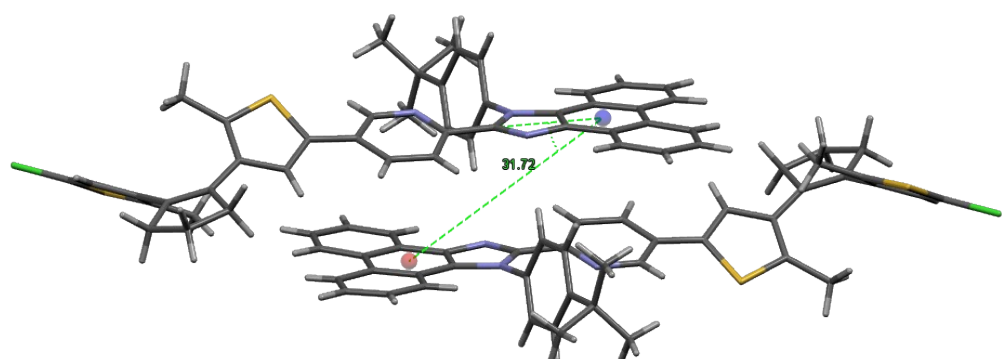


Fig. S8. The slip angle in molecular dimer of **BTE-P1**.

Table S3. Crystallographic data for **BTE-P1**.

Compound BTE-P1 (CCDC No. 2021742)			
Empirical formula	C ₄₅ H ₃₈ ClN ₃ S ₂	F (000)	756.0
Formula weight	720.35	Crystal size (mm)	0.50 × 0.29 × 0.05
Crystal color	red	2θ range(°)	5.82 - 49.994
Temperature (K)	273.15	Limiting indices	-14 ≤ h ≤ 14, -15 ≤ k ≤ 15, -17 ≤ l ≤ 17
Wavelength (Å)	0.71073		
Crystal system	triclinic		
Space group	P-1	Reflections collected	48015
a (Å)	12.3552(16)	Independent reflections	6766
b (Å)	12.6875(16)	R _{int}	0.0347
c (Å)	14.5673(18)	Completeness to θ (%)	99.7 (θ = 24.997)
α (°)	102.375(4)	Goodness-of-fit on F ²	1.023
β (°)	115.070(4)	Final R indices [I > 2σ(I)]	R1 = 0.0538 wR2 = 0.1468
γ (°)	100.058(5)		
Volume (Å ³)	1927.3(4)	R indices (all data)	R1 = 0.0692 wR2 = 0.1619
Z	2		
D calcd (mg•m ⁻³)	1.241	Largest diff. peak and hole (e Å ⁻³)	0.86 and -0.50
μ (mm ⁻¹)	0.243		

Table S4. Fractional Atomic Coordinates ($\times 10^4$) and Equivalent Isotropic Displacement Parameters (Å² $\times 10^3$) for **BTE-P1**. U_{eq} is defined as 1/3 of the trace of the orthogonalised U_{ij} tensor.

Atom	x	y	z	U(eq)
Cl1	3200.6(12)	-3315.5(12)	10121.8(10)	122.6(4)
S1	3273.0(9)	-1155.0(9)	9631.7(7)	87.3(3)
S2	5909.0(6)	335.4(5)	7426.6(5)	51.99(19)
N3	7264.7(18)	5512.7(15)	6044.9(15)	44.5(4)
N2	6060.8(18)	4440.8(16)	4322.3(15)	47.3(5)
N1	6609(2)	3505.7(18)	6611.2(16)	58.0(6)
C5	8913(2)	6723(2)	9420(2)	58.3(6)

C6	7666(3)	6614(3)	8763(2)	62.3(7)
C7	9585(2)	6384(2)	8911(2)	62.5(7)
C8	7119(2)	6205(2)	7662(2)	53.8(6)
C9	9049(2)	5961(2)	7815(2)	56.0(6)
C10	7814(2)	5880.0(19)	7194.9(18)	44.2(5)
C11	9486(3)	9177(3)	6991(3)	84.4(10)
C12	8840(3)	8079(2)	6778(2)	67.7(7)
C13	9441(3)	9557(3)	6164(3)	84.1(10)
C14	8127(2)	7332(2)	5729(2)	50.2(6)
C15	8742(3)	8858(3)	5136(3)	71.6(8)
C16	8044(2)	7727(2)	4862(2)	54.7(6)
C17	7429(2)	6168.1(19)	5433.5(19)	45.3(5)
C18	6684(2)	5481(2)	4387.5(19)	45.5(5)
C19	7258(2)	7005(2)	3754(2)	56.1(6)
C20	7092(3)	7394(3)	2881(3)	76.7(9)
C21	6581(2)	5871(2)	3503(2)	51.0(6)
C22	6331(4)	6706(4)	1851(3)	90.9(11)
C23	5701(3)	5590(3)	1622(3)	84.6(10)
C24	5830(3)	5173(3)	2447(2)	65.6(7)
C25	6422(2)	4483.2(19)	5327.0(18)	43.8(5)
C26	5965(2)	3521.0(19)	5610.1(18)	43.9(5)
C27	6203(3)	2596(2)	6831(2)	58.6(7)
C28	4915(2)	2641.0(19)	4829.4(18)	46.2(5)
C29	5191(2)	1657.6(19)	6101.2(18)	45.8(5)
C30	4534(2)	1709(2)	5075.6(19)	47.5(5)
C31	4835(2)	665(2)	6385.8(19)	46.8(5)
C32	3703(2)	-141.1(19)	5908.7(19)	47.8(5)
C33	3668(2)	-1009.9(19)	6378.9(19)	46.1(5)
C34	4819(2)	-874.6(19)	7210.9(19)	47.0(5)
C35	5239(3)	-1631(2)	7862(2)	58.2(6)
C36	2518(2)	-1947.9(19)	5957(2)	48.5(6)
C37	1651(3)	-2434(2)	4764(2)	63.7(7)
C38	754(3)	-3511(3)	4629(3)	85.3(10)
C39	913(3)	-3462(2)	5715(3)	69.1(8)
C40	2069(2)	-2469(2)	6488(2)	51.6(6)
C41	2508(2)	-2186(2)	7641(2)	56.0(6)
C42	2891(3)	-16(2)	8150(3)	77.3(9)
C43	2852(3)	-1125(2)	8348(2)	64.1(7)
C44	2579(3)	-3026(3)	8166(3)	69.8(8)
C45	2976(3)	-2583(3)	9224(3)	82.6(10)
C1	9548(3)	7199(3)	10636(2)	87.1(11)
C2	8755(4)	7662(5)	11052(3)	140(2)

C3	10675(5)	8257(5)	11024(4)	161(2)
C4	10173(7)	6452(6)	11145(4)	187(3)

Table S5. Anisotropic Displacement Parameters ($\text{\AA}^2 \times 10^3$) for **BTE-P1**. The Anisotropic displacement factor exponent takes the form: $-2\pi^2[h^2a^*{}^2U_{11}+2hka^*b^*U_{12}+\dots]$.

Atom	U11	U22	U33	U23	U13	U12
C11	128.5(9)	175.6(12)	125.5(9)	106.4(9)	76.6(8)	75.3(9)
S1	94.3(7)	106.8(7)	71.3(5)	28.5(5)	48.4(5)	32.2(5)
S2	47.0(4)	50.3(4)	52.0(4)	22.5(3)	17.9(3)	7.3(3)
N3	46.2(11)	43.8(10)	42.7(10)	18.4(8)	19.2(9)	11.4(9)
N2	51.7(12)	48.2(11)	43.3(11)	19.4(9)	22.1(9)	14.3(9)
N1	60.7(13)	52.0(12)	45.1(11)	22.1(10)	13.5(10)	2.6(10)
C5	53.6(15)	59.9(15)	47.9(14)	7.9(12)	17.1(12)	16.9(12)
C6	54.2(16)	82.7(19)	51.0(15)	15.1(14)	26.2(13)	28.0(14)
C7	43.5(14)	74.2(18)	53.8(15)	11.6(13)	12.9(12)	19.9(13)
C8	43.4(13)	66.0(16)	50.8(14)	19.7(12)	19.7(11)	20.4(12)
C9	45.4(14)	68.5(16)	52.4(15)	14.7(12)	22.3(12)	22.1(12)
C10	44.9(13)	40.8(12)	44.2(12)	16.8(10)	18.0(10)	11.6(10)
C11	88(2)	53.8(17)	89(2)	13.7(16)	35.3(19)	0.6(16)
C12	74.0(19)	51.9(15)	70.1(18)	19.7(14)	32.2(16)	8.5(14)
C13	79(2)	54.4(17)	114(3)	33.8(19)	45(2)	5.2(16)
C14	44.6(13)	48.0(13)	64.8(16)	24.6(12)	28.1(12)	16.5(11)
C15	66.1(18)	65.0(18)	104(3)	47.7(18)	48.8(19)	20.4(15)
C16	47.6(14)	56.9(15)	76.9(18)	36.3(14)	35.9(14)	21.2(12)
C17	44.5(13)	46.2(12)	52.9(14)	23.6(11)	25.4(11)	16.6(10)
C18	47.8(13)	47.9(13)	49.3(13)	23.2(11)	25.8(11)	18.0(11)
C19	55.2(15)	67.6(16)	71.1(17)	41.2(14)	40.1(14)	28.0(13)
C20	81(2)	88(2)	89(2)	57(2)	50.7(19)	26.9(18)
C21	51.2(14)	65.0(16)	55.1(15)	32.4(13)	32.1(12)	26.6(12)
C22	100(3)	123(3)	78(2)	66(2)	51(2)	33(2)
C23	97(2)	109(3)	58.1(18)	41.6(19)	40.8(18)	26(2)
C24	73.3(19)	78.9(19)	55.1(16)	31.5(15)	35.1(15)	23.2(15)
C25	44.5(12)	44.7(12)	42.2(12)	17.6(10)	18.9(10)	13.3(10)
C26	48.2(13)	45.7(12)	42.0(12)	19.2(10)	22.3(11)	15.5(10)
C27	62.1(16)	56.2(15)	44.1(13)	24.6(12)	14.5(12)	5.2(12)
C28	48.2(13)	49.1(13)	41.0(12)	17.5(10)	19.6(11)	14.5(11)
C29	46.6(13)	45.6(12)	47.1(13)	17.2(10)	23.5(11)	12.2(10)

C30	48.1(13)	44.6(12)	45.0(13)	14.3(10)	19.9(11)	9.1(10)
C31	49.9(14)	45.8(13)	47.3(13)	18.4(11)	24.2(11)	14.3(11)
C32	45.3(13)	49.2(13)	49.2(13)	20.2(11)	20.5(11)	14.8(11)
C33	46.4(13)	44.4(12)	52.5(13)	17.3(11)	27.0(11)	14.5(10)
C34	49.5(14)	42.7(12)	51.2(13)	17.4(10)	25.7(11)	12.3(10)
C35	56.0(15)	56.0(15)	66.1(16)	30.7(13)	26.7(13)	18.2(12)
C36	44.2(13)	42.2(12)	58.0(14)	14.2(11)	24.1(11)	13.6(10)
C37	54.1(16)	61.9(16)	62.6(17)	14.6(13)	22.4(13)	9.8(13)
C38	70(2)	71(2)	81(2)	2.9(17)	27.5(18)	-7.4(16)
C39	59.0(17)	53.8(16)	87(2)	15.4(15)	36.8(16)	4.6(13)
C40	50.2(14)	40.4(12)	69.8(16)	17.9(12)	33.5(13)	13.5(11)
C41	51.8(15)	53.4(15)	73.5(17)	25.2(13)	37.3(13)	15.5(12)
C42	94(2)	57.1(17)	93(2)	16.1(16)	58(2)	25.0(16)
C43	67.7(18)	65.2(17)	69.7(18)	20.5(14)	42.0(15)	21.8(14)
C44	66.4(18)	69.8(18)	95(2)	40.3(17)	49.7(18)	23.3(15)
C45	73(2)	117(3)	89(2)	60(2)	50.2(19)	39(2)
C1	79(2)	109(3)	48.8(17)	4.6(17)	15.5(16)	35(2)
C2	104(3)	209(5)	68(2)	-14(3)	41(2)	31(3)
C3	107(4)	179(5)	118(4)	-36(3)	47(3)	-16(3)
C4	262(7)	219(6)	72(3)	54(3)	47(3)	134(5)

Table S6. Bond Lengths for **BTE-P1**.

Atom	Atom	Length/Å	Atom	Atom	Length/Å
Cl1	C45	1.720(3)	C19	C21	1.414(4)
S1	C43	1.727(3)	C20	C22	1.361(5)
S1	C45	1.700(4)	C21	C24	1.389(4)
S2	C31	1.731(2)	C22	C23	1.383(5)
S2	C34	1.727(2)	C23	C24	1.375(4)
N3	C10	1.441(3)	C25	C26	1.467(3)
N3	C17	1.392(3)	C26	C28	1.387(3)
N3	C25	1.378(3)	C27	C29	1.386(3)
N2	C18	1.369(3)	C28	C30	1.371(3)
N2	C25	1.322(3)	C29	C30	1.389(3)
N1	C26	1.339(3)	C29	C31	1.462(3)
N1	C27	1.333(3)	C31	C32	1.363(3)
C5	C6	1.389(4)	C32	C33	1.421(3)
C5	C7	1.391(4)	C33	C34	1.373(3)
C5	C1	1.522(4)	C33	C36	1.472(3)
C6	C8	1.379(4)	C34	C35	1.496(3)
C7	C9	1.374(4)	C36	C37	1.511(4)

C8	C10	1.367(3)	C36	C40	1.340(3)
C9	C10	1.376(3)	C37	C38	1.519(4)
C11	C12	1.374(4)	C38	C39	1.495(5)
C11	C13	1.375(5)	C39	C40	1.515(4)
C12	C14	1.399(4)	C40	C41	1.466(4)
C13	C15	1.357(5)	C41	C43	1.374(4)
C14	C16	1.426(3)	C41	C44	1.432(4)
C14	C17	1.441(3)	C42	C43	1.492(4)
C15	C16	1.413(4)	C44	C45	1.351(5)
C16	C19	1.454(4)	C1	C2	1.492(5)
C17	C18	1.375(3)	C1	C3	1.554(6)
C18	C21	1.441(3)	C1	C4	1.454(6)
C19	C20	1.409(4)			

Table S7. Bond Angles for **BTE-P1**.

Atom	Atom	Atom	Angle/ [°]	Atom	Atom	Atom	Angle/ [°]
C45	S1	C43	91.41(15)	N2	C25	C26	122.3(2)
C34	S2	C31	92.84(11)	N1	C26	C25	118.5(2)
C17	N3	C10	126.02(19)	N1	C26	C28	122.2(2)
C25	N3	C10	127.70(18)	C28	C26	C25	119.3(2)
C25	N3	C17	106.17(18)	N1	C27	C29	125.3(2)
C25	N2	C18	104.95(19)	C30	C28	C26	119.3(2)
C27	N1	C26	117.1(2)	C27	C29	C30	116.1(2)
C6	C5	C7	116.6(2)	C27	C29	C31	122.3(2)
C6	C5	C1	123.1(3)	C30	C29	C31	121.6(2)
C7	C5	C1	120.3(3)	C28	C30	C29	120.0(2)
C8	C6	C5	122.0(2)	C29	C31	S2	121.62(18)
C9	C7	C5	122.0(2)	C32	C31	S2	109.51(17)
C10	C8	C6	119.4(2)	C32	C31	C29	128.8(2)
C7	C9	C10	119.4(2)	C31	C32	C33	114.9(2)
C8	C10	N3	119.4(2)	C32	C33	C36	121.7(2)
C8	C10	C9	120.5(2)	C34	C33	C32	111.8(2)
C9	C10	N3	120.0(2)	C34	C33	C36	126.4(2)
C12	C11	C13	119.9(3)	C33	C34	S2	110.92(17)
C11	C12	C14	121.3(3)	C33	C34	C35	130.1(2)
C15	C13	C11	120.2(3)	C35	C34	S2	118.90(18)
C12	C14	C16	119.2(2)	C33	C36	C37	119.6(2)
C12	C14	C17	125.0(2)	C40	C36	C33	129.4(2)
C16	C14	C17	115.7(2)	C40	C36	C37	111.1(2)
C13	C15	C16	122.7(3)	C36	C37	C38	104.0(2)
C14	C16	C19	121.5(2)	C39	C38	C37	107.2(2)

C15	C16	C14	116.6(3)	C38	C39	C40	105.0(2)
C15	C16	C19	121.9(2)	C36	C40	C39	110.8(2)
N3	C17	C14	131.7(2)	C36	C40	C41	129.7(2)
C18	C17	N3	105.1(2)	C41	C40	C39	119.5(2)
C18	C17	C14	123.0(2)	C43	C41	C40	126.1(2)
N2	C18	C17	111.56(19)	C43	C41	C44	111.3(3)
N2	C18	C21	126.6(2)	C44	C41	C40	122.6(3)
C17	C18	C21	121.8(2)	C41	C43	S1	111.8(2)
C20	C19	C16	122.8(3)	C41	C43	C42	129.5(3)
C20	C19	C21	116.5(3)	C42	C43	S1	118.7(2)
C21	C19	C16	120.7(2)	C45	C44	C41	112.7(3)
C22	C20	C19	121.6(3)	S1	C45	C11	120.8(2)
C19	C21	C18	117.1(2)	C44	C45	C11	126.4(3)
C24	C21	C18	121.6(2)	C44	C45	S1	112.8(2)
C24	C21	C19	121.2(2)	C5	C1	C3	108.7(3)
C20	C22	C23	121.0(3)	C2	C1	C5	113.8(3)
C24	C23	C22	119.6(3)	C2	C1	C3	102.8(4)
C23	C24	C21	120.1(3)	C4	C1	C5	112.1(3)
N3	C25	C26	125.5(2)	C4	C1	C2	116.4(4)
N2	C25	N3	112.21(19)	C4	C1	C3	101.5(5)

Table S8. Hydrogen Atom Coordinates ($\text{\AA} \times 10^4$) and Isotropic Displacement Parameters ($\text{\AA}^2 \times 10^3$) for **BTE-P1**.

Atom	x	y	z	U(eq)
H6	7184	6824	9076	75
H7	10424	6445	9325	75
H8	6285	6151	7241	65
H9	9517	5731	7495	67
H11	9954	9661	7694	101
H12	8877	7829	7342	81
H13	9890	10296	6309	101
H15	8723	9135	4589	86
H20	7512	8138	3011	92
H22	6234	6990	1292	109
H23	5193	5126	915	102
H24	5413	4422	2299	79
H27	6633	2591	7530	70
H28	4474	2683	4146	55
H30	3835	1112	4556	57
H32	3006	-124	5320	57
H35A	6108	-1551	8084	87
H35B	4752	-2403	7438	87

H35C	5126	-1426	8482	87
H37A	2114	-2600	4382	76
H37B	1205	-1913	4504	76
H38A	-102	-3561	4151	102
H38B	944	-4168	4329	102
H39A	1031	-4158	5858	83
H39B	186	-3345	5773	83
H42A	2670	452	8612	116
H42B	2307	-140	7416	116
H42C	3720	352	8293	116
H44	2374	-3794	7815	84
H2A	8374	8126	10651	210
H2B	9266	8108	11794	210
H2C	8114	7049	10979	210
H3A	11263	8043	10812	241
H3B	11076	8572	11790	241
H3C	10380	8811	10710	241
H4A	9568	5854	11133	280
H4B	10790	6874	11873	280
H4C	10575	6136	10764	280

5. DFT theoretical calculations of BTE-P2.

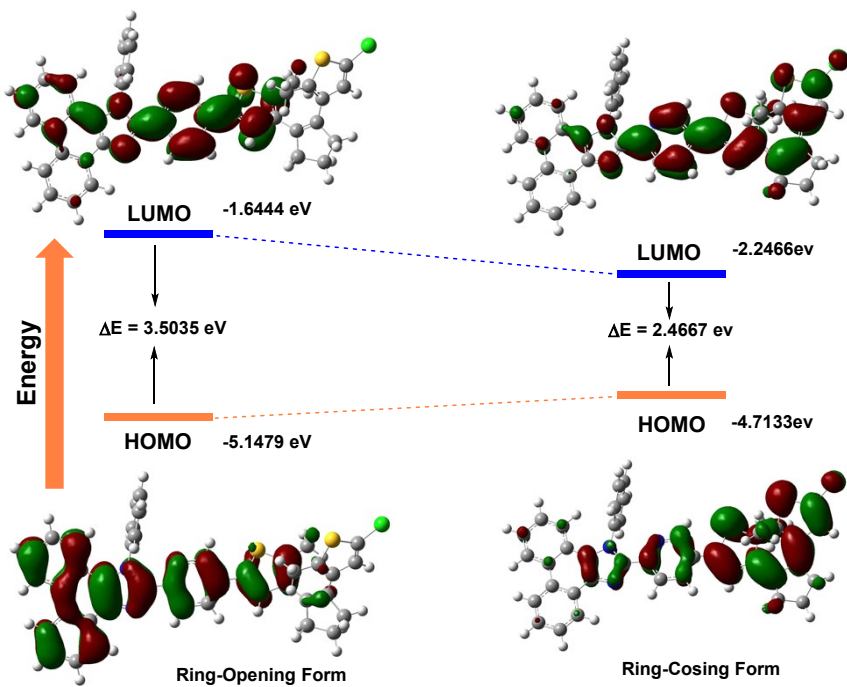


Fig. S9 Frontier molecular orbitals of **BTE-P2** by Gaussian 09 with the B3LYP/6-31G basis set.

6. Hydrodynamic diameters and photophysical properties of BTE-P1@DSPE-PEG2000.

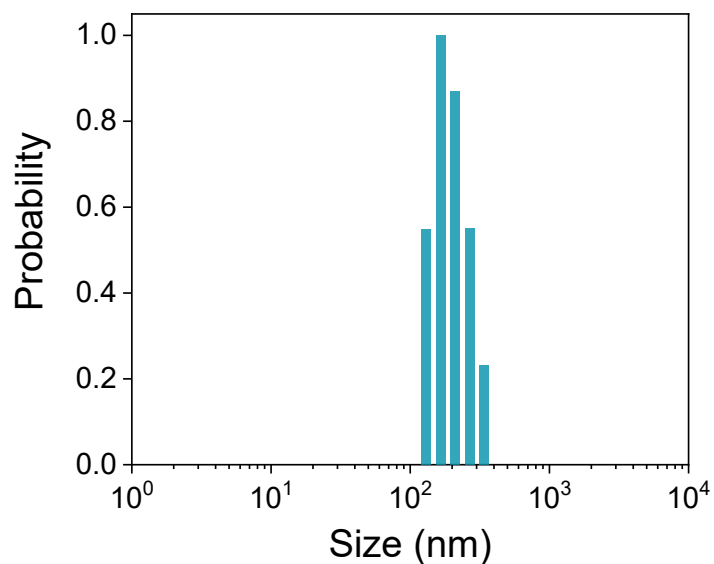


Fig. S10 Hydrodynamic diameters of BTE-P1@DSPE-PEG2000 at PBS buffer (pH

7.4)

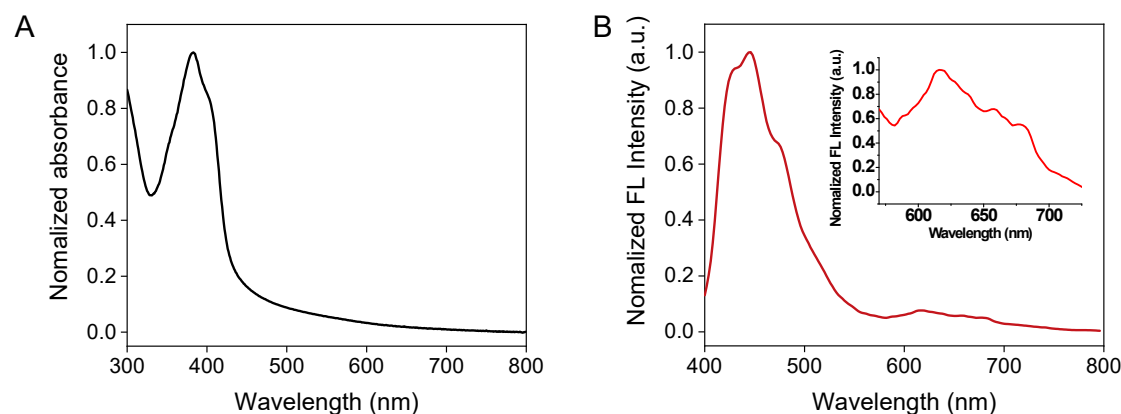


Fig. S11 Absorption (A) and fluorescence spectra (B, $\lambda_{\text{ex}} = 350$ nm) of BTE-P1@DSPE-PEG2000 in PBS buffer (pH 7.4)

7. Appendix: NMR spectra.

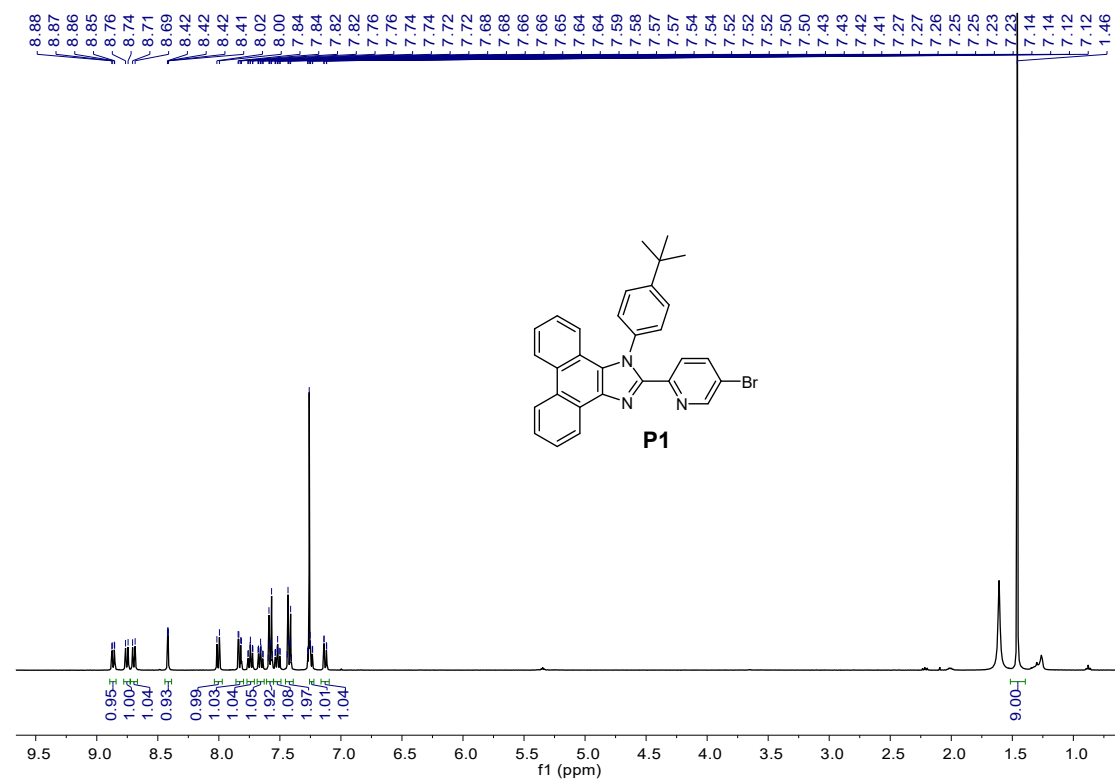


Fig. S12. ¹H NMR of P1

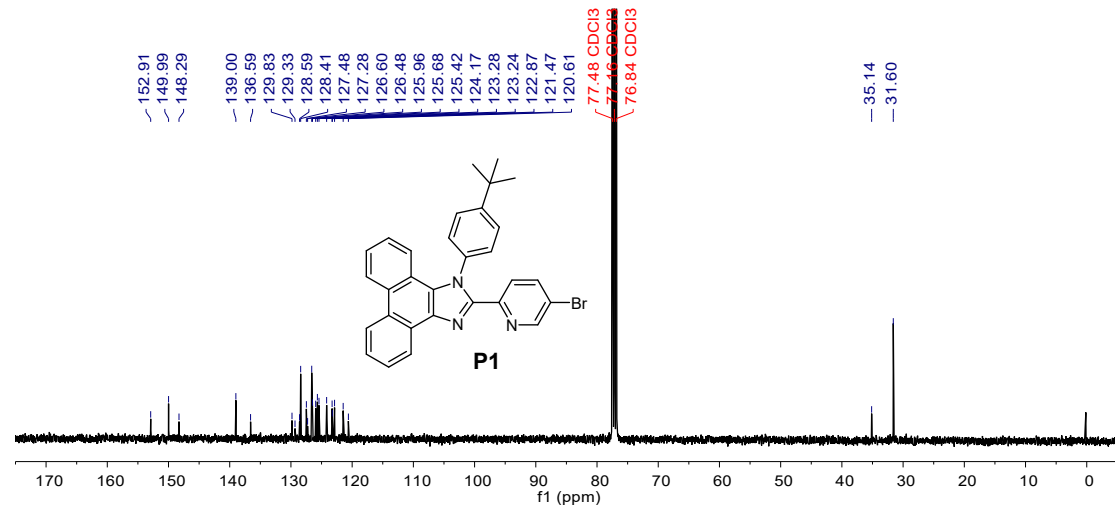


Fig. S13. ¹³C NMR of P1

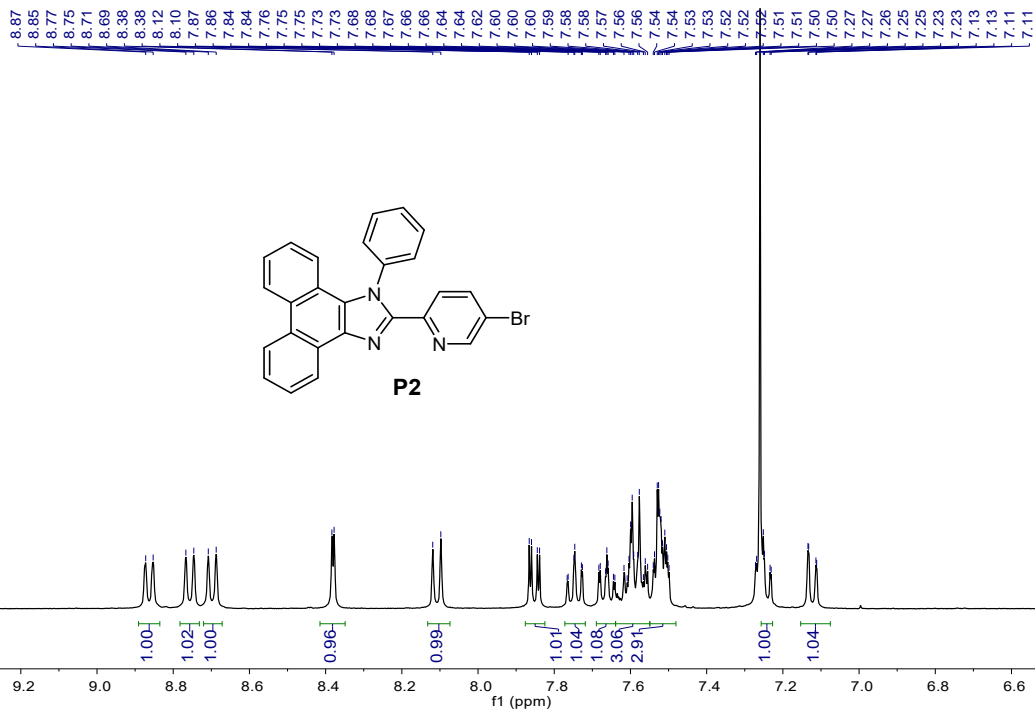


Fig. S14. ^1H MNR of **P2**

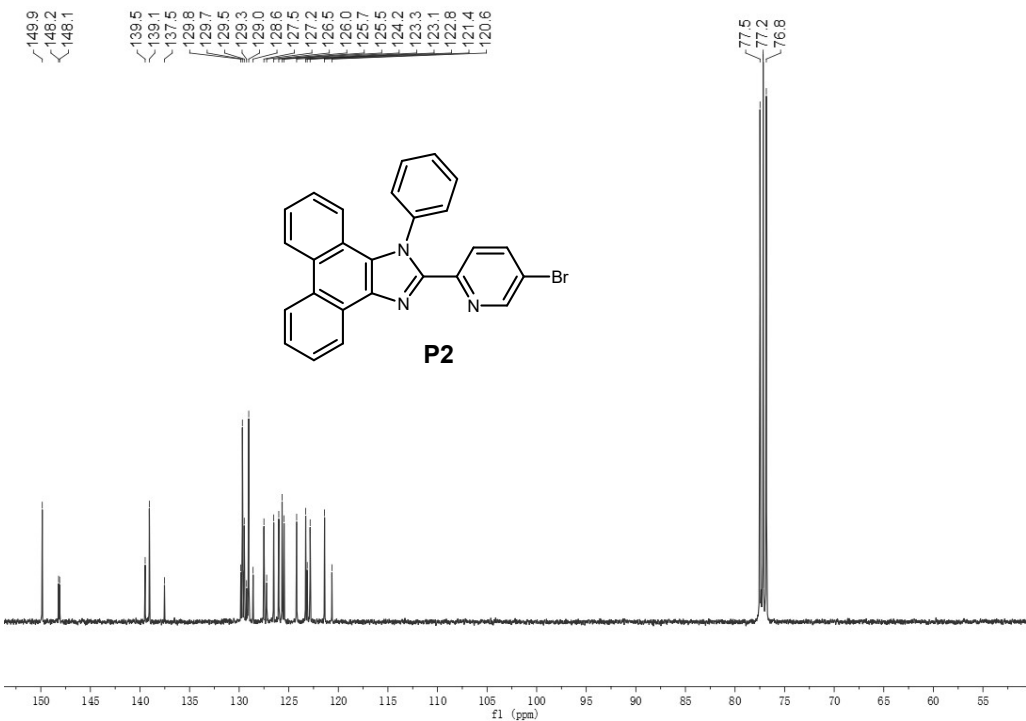


Fig. S15. ^{13}C MNR of **P2**

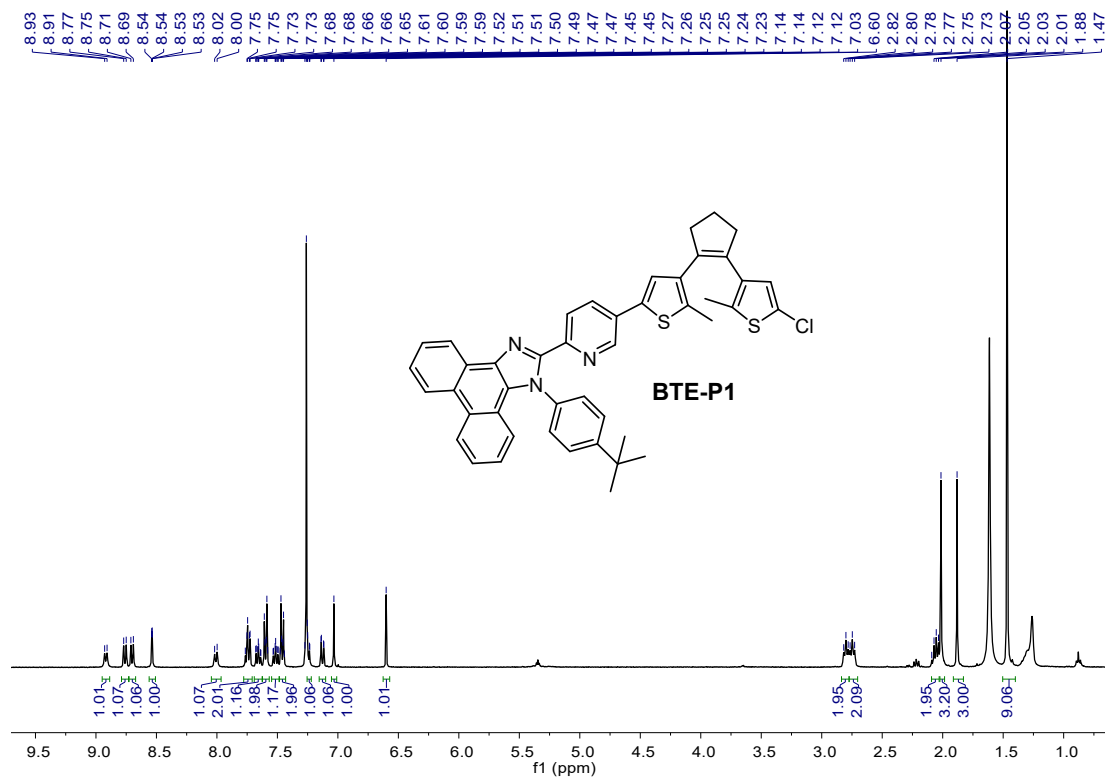


Fig. S16. ^1H MNR of BTE-P1

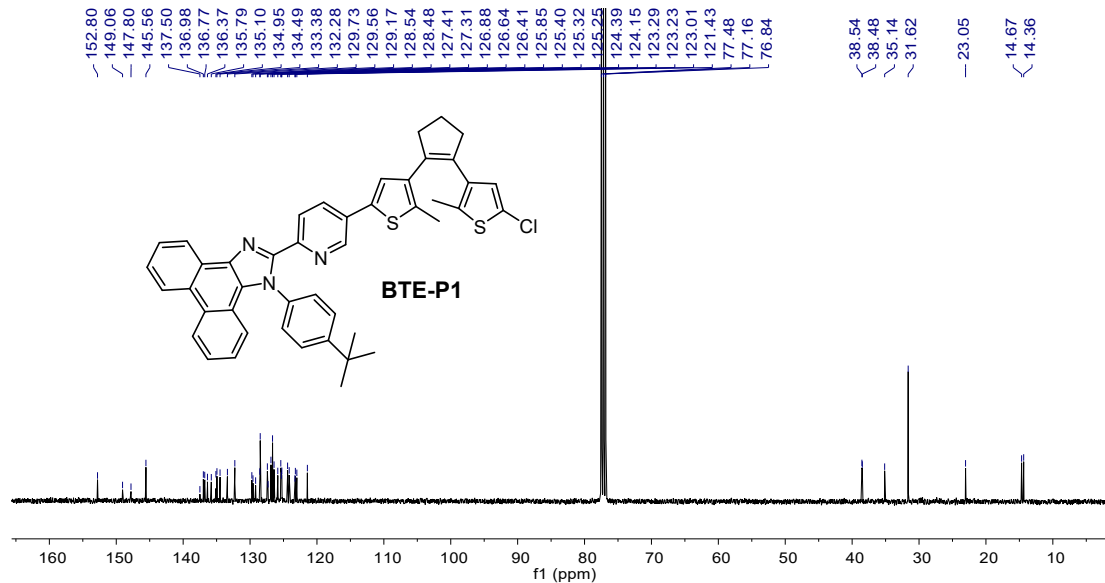


Fig. S17. ^{13}C MNR of BTE-P1

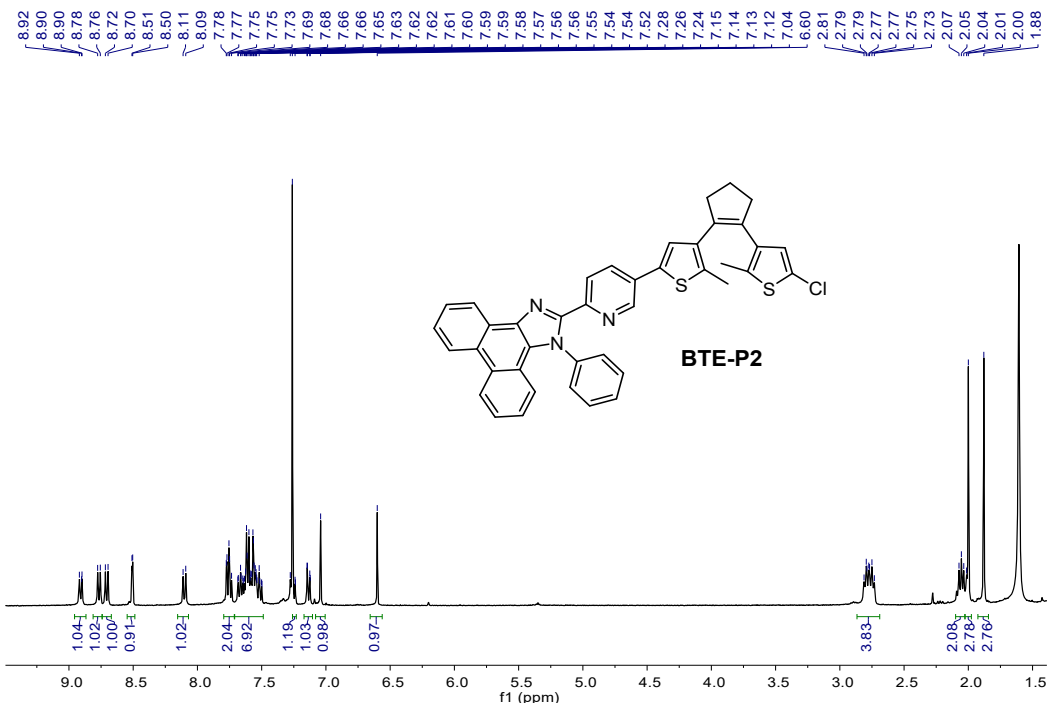


Fig. S18. ^1H MNR of BTE-P2

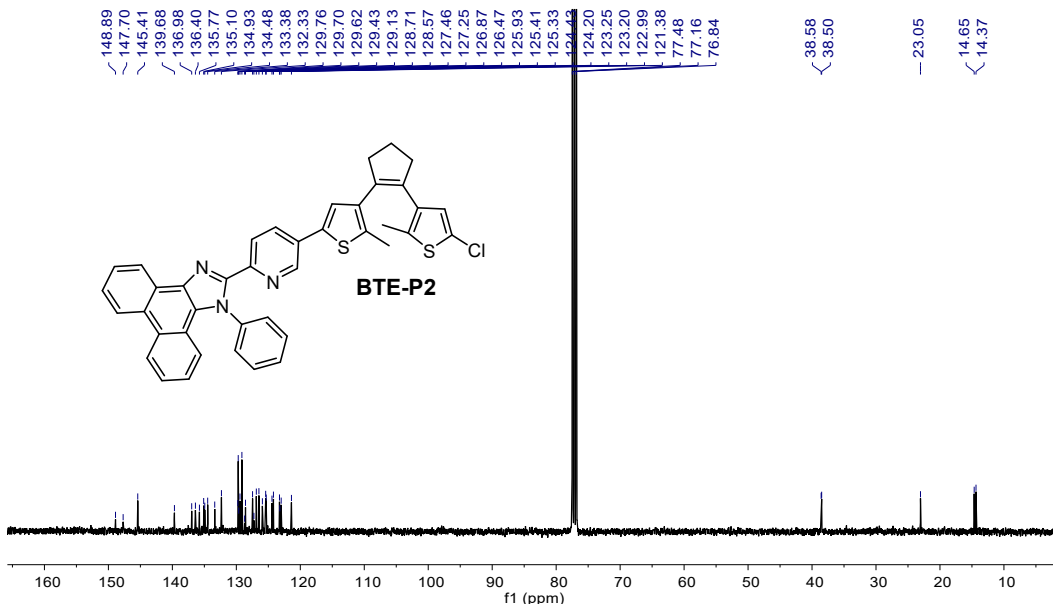


Fig. S19. ^{13}C MNR of BTE-P2

8. References

1. L. Ma, C. Li, Q. Yan, S. Wang, W. Miao and D. Cao, *Chin. Chem. Lett.*, 2020, **31**, 361-364.
 2. Y. Zhang, J.-H. Wang, J. Zheng and D. Li, *Chem. Commun.*, 2015, **51**, 6350-6353.